JOURNAL OF THEORETICAL AND APPLIED MECHANICS
45, 4, pp. 919-930, Warsaw 2007

ADAPTIVE VIBRATION CONTROL THROUGH A SMA EMBEDDED PANEL

Gianluca Diodati
Salvatore Ameduri
Antonio Concilio

The Italian Aerospace Research Centre, CIRA ScpA, Italy
e-mail: g.diodati@cira.it; s.ameduri@cira.it; a.concilio@cira.it

Dynamic behavior of structural elements and their performance in terms of noise and vibration control may be remarkably affected by several parameters, like geometry, material properties, stress field, etc. Ability of adaptively controlling one or more of these parameters leads to a structure fitting different requirements in several working conditions. Research activities presented in this work are focused on the design of a fiberglass laminate structural element with SMA wires embedded along the widest dimension. SMA contraction by the Joule effect heat adduction leads, if suitably constrained on the edges, to an internal stress field with a consequent over-all stiffness increase. The finite element code MSC.NASTRAN is used to simulate the whole system made of a plate and SMA wires controlling elements. The behavior of the SMA is modeled through the NASTRAN card CELAS that allows one to consider the additional SMA activation stiffness with a suitable "spring" constant, depending on the wire temperature and a suitable discretization parameter. The finite difference model of the SMA is achieved and integrated in the FEM solver.

Key words: SMA, embedding, vibration

1. Introduction

The ability of affecting the dynamic response of a structure, so that its performance in terms of noise and vibration control could fit several working conditions, represents a challenging objective. Due to the limitations of practical conventional solutions and due to the impossibility of producing significant

changes of the main structural features, innovative materials and design strategies have well done for themselves. According to this trend, the search for non-conventional materials oriented to the actuation to satisfy control performance requirements has been the main task during the past years. Among all, NiTi Shape Memory Alloys (SMAs) with their abilities to change their material properties such as Young's modulus (Ford and White, 1996; Otsuka and Wayman, 1998), damping capacity (Gandhi and Wolons, 1999; Piedboeuuf *et al.*, 1998), and the generation of large internal forces (Rogers *et al.* 1989), have found many applications. The idea of embedding SMA actuators in a composite laminate for structural control was first introduced by Rogers and Robertshaw [Rogers *et al.* 1988]. Such a structure was termed a Shape Memory Alloy Hybrid Composite (SMAHC).

The "Smart Structure & Material" concept and related properties may be used to make up for unsatisfactory dynamic characteristics, usually referred to natural frequencies and mode shapes; moreover, the design of a structure which is known to experience a dynamic working environment needs to satisfy some defined criteria such as averting vibration resonances in a variable load environment.

Shift of natural frequencies away from resonance conditions, shift of an antiresonance to a selected frequency for an assigned FRF, pole-zero cancellations, no resonance frequency range creation, may be achieved by precise tuning of SMA components in SMAHCs (Fuller *et al.*, 1996; Rogers *et al.*, 1989).

Rogers *et al.* (1989) presented concepts of using SMA wires for control of natural frequencies and modes of vibration of the simply supported plate but only examined SMA/Epoxy composite plates, for which the relative volume fraction of SMA wires was very high.

Changes in natural frequencies of clamped-clamped composite beams with SMA wires were investigated analytically and experimentally by Baz *et al.* (1995). Natural frequencies of composite beams modified in this manner were also significantly affected, but a very low thickness-to-length ratio was adopted.

It was shown that for a beam with SMA fibres with a nitinol volume of 15% the first natural frequency of the beam increased from 21 to 62 Hz, by heating the SMA wires from the room temperature up to 149°C (Rogers *et al.*, 1991).

Ostachowicz *et al.* 1998 investigated more general SMA composites paying attention to factors which influence the composite performance: the ratio of the SMA/reinforcing fibres Young's modulus ratio, the relative volume fraction of the SMA components, the relative volume fraction of the reinforcing fibres, the

structure thickness-to-length ratio, the location and orientation of the SMA components within the structure, and so on.

Two methods have been proposed for integrating SMA actuators into a composite: bonding the actuators within the composite matrix as a constituent and embedding the actuators within sleeves through the laminate and attaching it at some convenient chosen point in order to eliminate high shearing stresses arising from their activation process. The first method gives rise, from a control point-of-view, to the Active Property Tuning method, which exploits only changes in the stiffness of SMA components during their activation, while the second one to the so called Active Strain Energy Tuning method, which exploits the high recovery stress generated during activation of the SMA elements.

Various methodology, in the framework of Finite Element Analysis (FEA), have been proposed to simulate the behaviour of the SMAHC, differing for the underlying assumptions. One method is to develop special composite elements. This has been done for multi-layered composite plates (Lagoudas *et al.*, 1997; Ostachowicz *et al.*, 1998; Zak *et al.*, 2003) and for layered beams (Marfia *et al.*, 2003). A more general way is to model the matrix and reinforcing members separately (Gao *et al.*, 2004; Ghomshei *et al.*, 2001; Sun *et al.*, 2002).

The present paper is organized as in the following. Section 2 describes a numerical specimen that has been simulated and analyzed through the MSC.NASTRAN code. Section 3 presents numerical models used in the simulation. Section 4 illustrates results concerning a preliminary estimate focused on the stiffness increase of a single wire due to activation. Lastly, Section 5 collects related results in terms of the dynamic response of the system with and without wires activation. Furthermore, the dependence of the dynamic behaviour with respect to the number of SMA wires and different initial stress conditions are presented.

2. Main features of the numerical specimen

Numerical investigations illustrated in the following paragraphs have been performed on a ply-angle symmetric hybrid composite panel with planar dimension of 330×210 mm. Constituted by twelve 0.3 mm thick glass fiber reinforced epoxy plies disposed according to a stacking sequence of $[\pm 45_3^G]_S$ and characterized by a fiber volume ratio of 0.2, the specimen has been integrated by SMA wires inserted into sleeves embedded within the mid-surface and running along the plate widest dimension.

The wires are free to move within the sleeves but fixed on both the ends. Due to this design choice, no shear stresses are transmitted by the structure to the wires, with a consequent easier activation, and no local instability problems (buckling, wrinkling,...) may occur, being laminate in-plane displacements not enforced by wires contraction. The material and geometrical properties of the panel are summarized in Table 1. The properties of the SMA adopted are listed in Table 2. Figure 1 shows the physical arrangement considered in the numerical simulation.

Table 1. Geometry and physical constants for the panel

Parameter	Value	Parameter	Value
Dimensions	$L_x \times L_y = 330\,\text{mm} \times 210\,\text{mm}$	Poisson ratio resin	0.35
Thickness	$12 \cdot 0.3\,\text{mm} = 3.6\,\text{mm}$	Mass density fibres	$2250\,\text{Kg/m}^3$
Stacking sequence	$[\pm 45_3^G]_S$	E fibres	65.5 GPa
Mass density resin	$1250.0\,\text{Kg/m}^3$	Poisson ratio fibres	0.23
E resin	3.43 GPa	Vol. ratio of fibres	0.20

Table 2. Material properties of the nitinol alloy

Modul, density	Transformation temperatures	Transformation constants	Maximum residual strain
$E_A = 67.0\,\text{GPa}$	$M_F = 9.0°\text{C}$	$C_M = 8.0\,\text{MPa/°C}$	$\varepsilon_L = 0.067$
$E_M = 26.3\,\text{GPa}$	$M_S = 18.4°\text{C}$	$C_A = 13.8\,\text{MPa/°C}$	
$\theta = 0.55\,\text{MPa/°C}$	$A_S = 34.5°\text{C}$	$\sigma_S = 100.0\,\text{MPa}$	
$\rho = 6448.1\,\text{Kg/m}^3$	$A_F = 49.0°\text{C}$	$\sigma_F = 170.0\,\text{MPa}$	

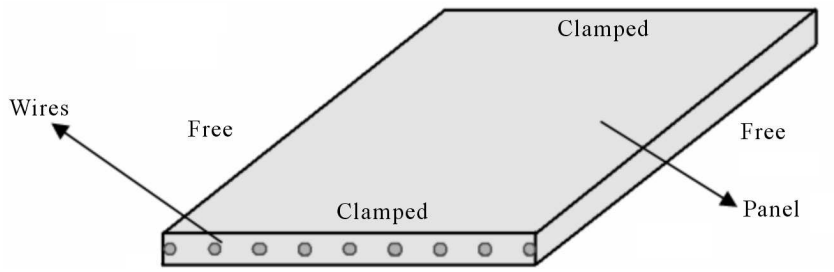

Fig. 1. The physical arrangement considered in simulations

3. Modeling strategy and numerical tools

Numerical investigations on the aforementioned specimen have been performed by adopting a FE approach.

The modeling of the panel has been carried out through the FEMAP 9.0 preprocessor, while numerical predictions in terms of mode shapes and modal frequencies up to a value of 1000 Hz have been achieved by the MSC/NASTRAN solver.

A right-handed Cartesian coordinate system has been chosen for the global FE space. The origin of the global coordinate system has been located on a panel corner. The X-direction has been chosen along the widest dimension and the Z-direction orthogonal to the specimen mid-surface.

6400 CQUAD elements (100 along X and 64 along Y directions) have been used to represent the plate. The 2D-orthotropic material nature has been defined through the PCOMP element card.

To take into account the additional mass and stiffness due to the SMA wires, 200 elements for each wire (in the simulation several numbers of wires have been considered) have been added to the model, to subtract the composite properties and to add the SMA properties.

To model the SMAs actuators, a Finite Difference (FD) scheme that can be included in the Finite Element code through the CELAS card has been used. The mechanism responsible for the shape recovery is a phase transformation of the SMA material from martensite to austenite. In the martensitic phase, the SMA is relatively soft and can be plastically deformed with low stress levels. As the alloy is heated, austenitic transformation occurs between a certain temperature range. The phase transformation from martensite to austenite is associated with a strain recovery process. If suitable constraint conditions are imposed, a stress field occurs inside the SMA elements during the recovery. To be able to predict the deformation behavior of a structure subjected to SMA-induced forces, the interaction of the SMA wire with the structure needs to be clearly understood as well as the thermo-mechanical constitutive modeling involved in the strain recovery of the SMA.

The Brinson model (Brinson, 1993; Rogers *et al.*, 1991) has been adopted as the thermo-mechanical model of the SMA. The constitutive law is the generalized Hooke law

$$\sigma = \sigma_0 + D(\xi)\varepsilon - D(\xi_0)\varepsilon_0 - \varepsilon_L D(\xi)\xi_s + \varepsilon_L D(\xi_0)\xi_{s0} + \theta(T - T_0) \tag{3.1}$$

where σ, ε, T represent the actual stress, strain and temperature, the symbol $(\cdot)_0$ denotes related initial values, θ – the thermoelastic coefficient. It is

assumed that Young's modulus D is a function of the martensite volume fraction ξ. The function to describe the martensite volume fraction ξ is defined as the sum of two fractions

$$\xi = \xi_S + \xi_T \tag{3.2}$$

where ξ_S and ξ_T describe stress and temperature-induced martensite volume fractions, respectively. Further details on the model can be found in Zak *et al.* (2003).

The dynamic properties of the plate can be predicted as a function of temperature of the SMA wire. Assuming the initial and total strain in the wire (ε_0 and ε values), temperature of the wire T and the initial strain σ_0, residual equation (3.1) may be solved in terms of σ; related axial force F inside the wire may be derived (no interaction between the wire and the panel are allowed in the activation phase). From the tension F, the effect of actuators on the structure may be calculated. The wires within the sleeves behave like a string governed by the equation

$$m\frac{d^2w(x,t)}{dt^2} - F\frac{d^2w(x,t)}{dx^2} = f(x,t) = f_m(x,t) + f_k(x,t) \tag{3.3}$$

where m is the wire mass per unit length, w – the vertical displacement of the wire and F – the tension. The force acting on the structure due to the SMA wire is represented by the term $-f(x,t)$. The mass effects of the wire is taken into account by adding additional beam elements to the plate FE model (the term $-f_m(x,t) = -md^2w(x,t)/dt^2$), but the most important change in the structure is caused by the mechanical coupling between the string and the plate subsystems ($-f_k(x,t) = Fd^2w(x,t)/dx^2$). Basing on the finite difference scheme, this force can be expressed by the following equation

$$f_i^{plate} = -f_k(x_i,t)\Delta l = \frac{F}{\Delta l}(w_{i+1} - w_i) - \frac{F}{\Delta l}(w_i - w_{i-1}) \tag{3.4}$$

the MSC/NASTRAN CELAS card may be used to add the two contributions of equation (3.4) if a suitable spring constant $F/\Delta l$ is adopted.

The FE model has been tested through a theoretical model developed for a beam-like structure clamped at both ends (see Diodati and Ameduri [4]). Neglecting the bending stiffness of the string, the natural frequencies of the system are the zeros of the following equation

$$\cos(k_2 L) - \frac{1}{\cosh(k_1 L)} - \beta^2 \sin(k_2 L)\tanh(k_1 L) = 0 \tag{3.5}$$

In Fig. 2a, the first four beam natural frequencies of the system are plotted, while in Fig. 2b the shift of these frequencies for SMA wire tension between

0 N and 110 N is illustrated. The maximum relative error of 2.5%, when the internal force is 110 N, shows a good agreement between the numerical and theoretical models.

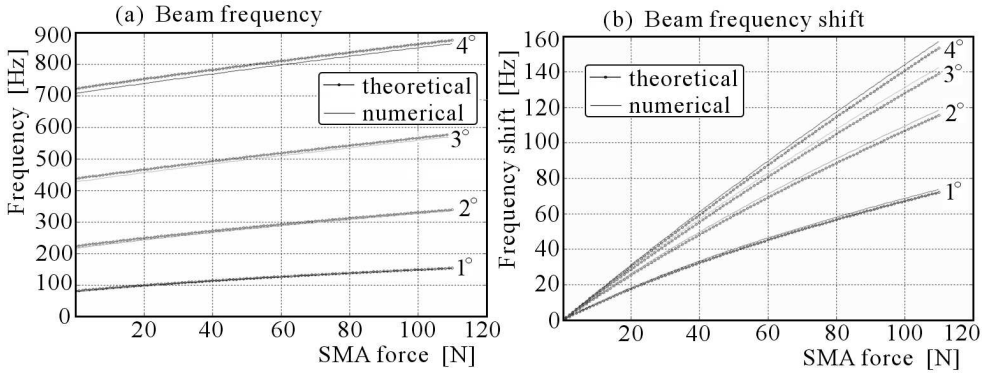

Fig. 2. Natural frequencies of the beam – comparison of numerical and theoretical results

4. Estimate of stiffness increase of a single wire

To have an idea of the SMA wires ability to affect the dynamic response and increase stiffness, the abovementioned SMA model has been adopted to estimate the single wire modes shift, before evaluating its effect on the surrounding structure.

More in detail, by hindering each deformation of the wire, the axial load P has been estimated vs. temperature. The frequency shift has been evaluated by Blevins *et al.* (1995)

$$f_i = \Big(\frac{i^2\pi^2}{2\pi L^2}\Big)\sqrt{1+\frac{PL^2}{i^2\pi^2 EI}}\sqrt{\frac{EI}{m}} \tag{4.1}$$

where i, L, m, I, E represent the mode id., the wire length, the mass per unit length, the cross section inertia moment and the Young modulus. No initial stress has been imposed. The first 10 modes shifts vs. temperature and axial stress have been plotted in Fig. 3. A temperature increase of 40°C, has determined an arise of the first mode from 7.48 us to 229.2 Hz.

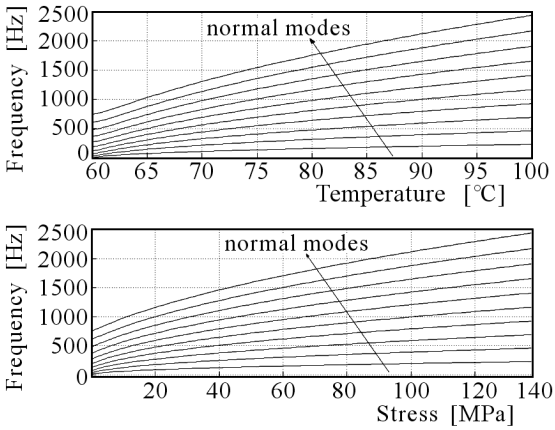

Fig. 3. Frequency shift in a single wire

5. Numerical results

Numerical calculations have been carried out for examination of SMA wires actuation effect on dynamic characteristics of the plate. As the first example, some results for the influence of SMA wires number are presented in Fig. 4. Increasing the number of SMA wires results in increasing the weight of the plate that hinders the natural frequencies from shifting towards higher values.

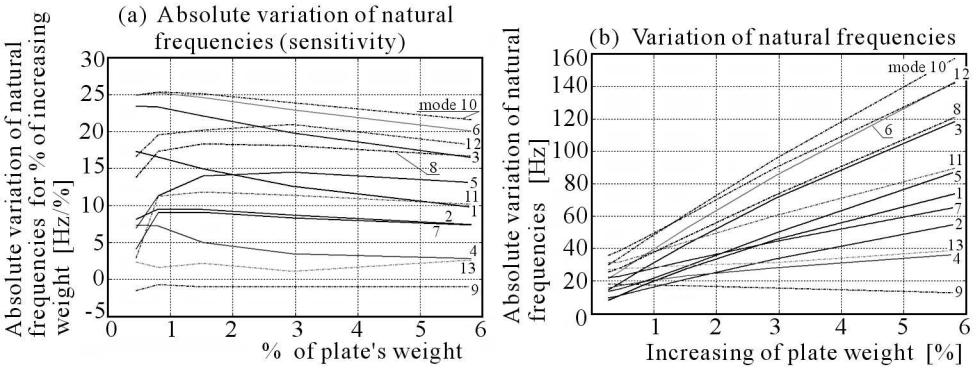

Fig. 4. Effect of increasing the number of SMA wires

The study shows that with a very limited increase in weight, one can reach a sensible shift of all natural frequencies of the plate (up to 160 Hz). All the modes are affected by the actuation, but the best performance is observed for modes for which the nodal lines are perpendicular to the orientation angle

of SMA wires (Fig. 4b). The sensitivity study has proved that the frequency shift is a quasi-linear function of the wires number: the SMA control system $[df/d(weight)]$ does not undergo saturation (Fig. 4a).

The initial stress and strain conditions (Fig. 5) have proved to strongly affect the SMA temperature influence on dynamic characteristics: the larger is the initial stress, the lower is the frequency shift. The initial strain has to be kept as small as possible to have the final activation temperature lower than the resin cure one.

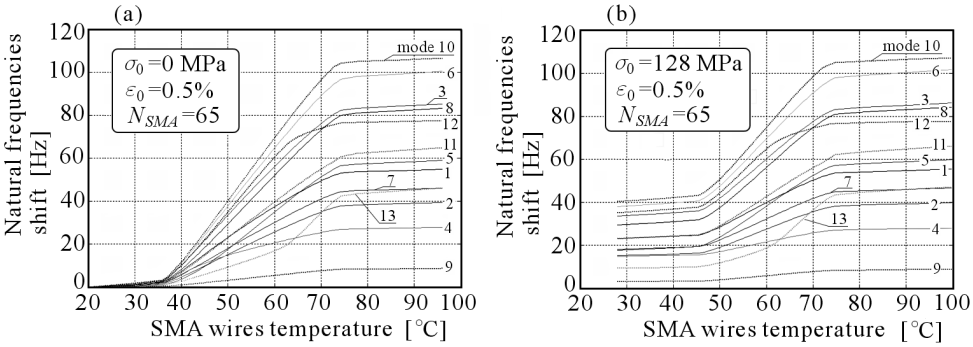

Fig. 5. Effect of increasing the temperature of SMA wires for different initial conditions

FRF curves plotted in Fig. 6 show that large peaks and anti-resonance shift may be obtained only in the transformation temperature range (i.e. 36-74°C and 45-75°C for the initial stress of 0 MPa (Fig, 6a) and 128 MPa (Fig. 6b), respectively).

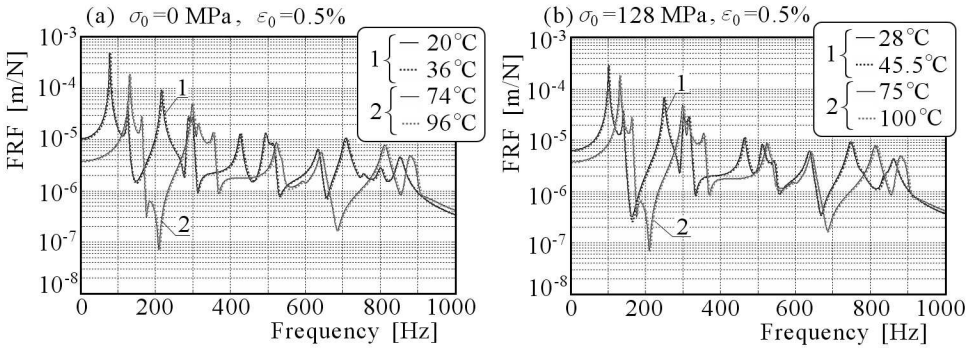

Fig. 6. Effect of increasing the temperature of SMA wires: FRF data

6. Conclusions and further steps

In the present paper, design and implementation of a numerical model aimed at describing the dynamic behavior of an anisotropic plate controlled by embedded SMA wires has been described. The stress field due to contraction of SMA wires constrained at the edges has been used for increasing the over-all stiffness. The numerical model has been obtained by adopting a finite difference approach aimed at estimating the stiffness increase due to activation of the axial load, predicted by the Brinson model. The achieved results have been presented in terms of frequency shift of both the single wire and the entire structure. Further efforts will be spent on the modeling of structure controlled by SMA wires. The aforementioned model will be compared with another one, describing the stiffness increase through an additional stiffness contribution (axial load geometric stiffness). Experimental campaigns are being carried out to validate the numerical predictions.

References

1. Baz A., Poh S., Ro J., Gilheany J., 1995, Control of the natural frequencies of nitinol-reinforced composite beams, *Journal of Sound and Vibration*, **185**, 1, 171-185

2. Blevins R.D., 2001, *Formulas for Natural Frequency and Mode Shape*, Krieger Publishing Company, Malabar Florida, p. 144

3. Brinson L.C., 1993, One-dimensional constitutive behavior of shape memory alloys: thermomechanical derivation with non-constant material functions and redefined martensite internal variable, *Journal of Intelligent Material Systems and Structures*, **4**, 2, 229-242

4. Diodati G., Ameduri S., Natural Frequencies of a Coupled Beam-String System, Technical Report CIRA-TR-06-0187

5. Ford D.S., White S.R., 1996, Thermomechanical behaviour of 55Ni45Ti nitinol, *Acta Materialia*, **44**, 6, 2295-2307

6. Fuller C.R., Elliott S.J., Nelson P.A., 1996, *Active Control of Vibration*, Academic Press Ltd., London

7. Gandhi F., Wolons D., 1999, Characterization of the pseudoelastic damping behaviour of shape memory alloy wires using complex modulus, *Journal of Smart Material Structures*, **8**, 49-56

8. GAO X., BURTON D., BRINSON L.C., 2004, Finite element simulation of a self-healing shape memory alloy composite, *Mechanics of Materials*, in press

9. GHOMSHEI M.M., KHAJEPOUR A., TABANDEH N., BEHDINAN K., 2001, Finite element modeling of shape memory alloy composite actuators: theory and experiment, *Journal of Intelligent Material Systems and Structures*, **12**, 11, 761-773

10. LAGOUDAS D.C., MOORTHY D., QIDWAY M.A., REDDY J.N., 1997, Modelling of the thermomechanical response of active laminates with SMA strips using the layerwise finite element method, *Journal of Intelligent Material Systems and Structures*, **8**, 6, 476-488

11. MARFIA S., SACCO E., REDDY J.N., 2003, Superelastic and shape memory effects in laminated shape memory alloy beams, *AIAA Journal*, **41**, 1, 100-109

12. OSTACHOWICZ W., KRAWCZUK M., ZAK A., 1998, Natural frequencies of multi-layer composite plate with embedded shape memory alloy wires, *Journal of Intelligent Material Systems and Structures*, **9**, 3, 232-237

13. OTSUKA K., WAYMAN C.M., 1998, *Shape Memory Materials*, Cambridge University Press, Cambridge

14. PIEDBOEUUF M.C., GAUVIN R., THOMAS M., 1998, Damping behaviour of shape memory alloys: strain amplitude, frequency and temperature effects, *Journal of Sound and Vibration*, **214**, 5, 885-901

15. ROGERS C.A., BAKER D.K., JAEGER C.A., 1989a, *Introduction to Smart Materials and Structures*, Smart Materials, Structures, and Mathematical Issues, Technomic Publishing Company, Inc.

16. ROGERS C.A., LIANG C., BAKER D.K., 1989b, *Dynamic Control Concepts Using Shape Memory alloy Reinforced Plates*, Smart Materials, Structures, and Mathematical Issues, Technomic Publishing Company, Inc.

17. ROGERS C.A., LIANG C., FULLER C.R., 1991, Modelling of shape memory alloy hybrid composites for structural acoustic control, *Journal of Acoustical Society of the America*, **89**, 210-220

18. ROGERS C.A., ROBERTSHAW H.H., 1988, *Shape Memory Alloy Reinforced Composite*, Engineering Science Preprints 25, Society of Engineering Science, Inc., ESP25.8027

19. SUN S.S., SUN G., WU J.S., 2002, Thermo-viscoelastic bending analysis of a shape memory alloy hybrid epoxy beam, *Smart Materials and Structures*, **11**, 6, 970-975

20. ZAK A., CARTMELL M., OSTACHOWICZ W., 2003a, Static and dynamic behaviour of composite structures with shape memory alloy components, *Materials Science Forum*, 440/441, 345-352

21. Zak A.J., Cartmell M.P., Ostachowicz W., 2003b, Dynamics of multilayered composite plates with shape memory alloy wires, *Journal of Applied Mechanics-Transactions of the ASME*, **70**, 3, 313-327

Adaptacyjne sterowanie drganiami w panelu zawierającym elementy ze stopu z pamięcią kształtu

Streszczenie

Właściwości dynamiczne elementów konstrukcyjnych oraz ich cechy rozważane pod kątem sterowalności drganiami i hałasem mogą być znacząco zmieniane takim parametrami jak geometria, właściwości materiałowe, pole naprężeń, itp. Zdolność do modyfikacji jednego lub więcej z wyżej wymienionych parametrów tworzy konstrukcję adaptowalną do różnych warunków pracy. Badania opisane w artykule dotyczą panelu wykonanego z laminatu wzmacnianego włóknem szklanym i dodatkowo zawierającego druty ze stopu z pamięcią kształtu (SMA) umieszczone wzdłuż największego wymiaru panelu. Kurczenie się stopu wywołane efektem Joule'a przy obecności źródła ciepła wytwarza wewnętrzne pole naprężeń, które prowadzi wprost do zwiększenia sztywności panelu. Do analizy całego układu laminowanej płyty i zatopionych drutów SMA użyto pakietu MSC.NASTRAN. Zachowanie SMA symulowano w pakiecie za pomocą karty CELAS, która pozwoliła na uwzględnienie dodatkowej sztywności od aktywacji SMA poprzez wprowadzenie nowej „sprężyny" o sztywności zależnej od temperatury oraz zadeklarowanego parametru dyskretyzacji. Model SMA wygenerowany metodą elementów skończonych poddano całkowaniu wewnątrz zastosowanego pakietu MES.

Manuscript received February 21, 2007; accepted for print April 4, 2007